Comparing and Combining Implicit Ligand Sampling with Multiple Steered Molecular Dynamics to Study Ligand Migration Processes in Heme Proteins

FLAVIO FORTI,[1] LEONARDO BOECHI,[2] DARIO A. ESTRIN,[2] MARCELO A. MARTI[2,3]
[1]*Department de Fisicoquimica and Institut de Biomedicina (IBUB), Facultat de Farmàcia, Universitat de Barcelona, Barcelona, Spain*
[2]*Departamento de Química Inorgánica, Analítica, y Química Física, INQUIMAE-CONICET, Facultad de Ciencias Exactas y Naturales Universidad de Buenos Aires. Ciudad Universitaria, Buenos Aires, Argentina*
[3]*Departamento de Química Biológica, Facultad de Ciencias Exactas y Naturales, Universidad de Buenos Aires. Ciudad Universitaria, Buenos Aires, Argentina*

Received 18 October 2010; Revised 18 January 2011; Accepted 6 March 2011
DOI 10.1002/jcc.21805
Published online in Wiley Online Library (wileyonlinelibrary.com).

Abstract: The ubiquitous heme proteins perform a wide variety of tasks that rely on the subtle regulation of their affinity for small ligands like O_2, CO, and NO. Ligand affinity is characterized by kinetic association and dissociation rate constants, that partially depend on ligand migration between the solvent and active site, mediated by the presence of internal cavities or tunnels. Different computational methods have been developed to study these processes which can be roughly divided in two strategies: those costly methods in which the ligand is treated explicitly during the simulations, and the free energy landscape of the process is computed; and those faster methods that use prior computed Molecular Dynamics simulation without the ligand, and incorporate it afterwards, called implicit ligand sampling (ILS) methods. To compare both approaches performance and to provide a combined protocol to study ligand migration in heme proteins, we performed ILS and multiple steered molecular dynamics (MSMD) free energy calculations of the ligand migration process in three representative and well theoretically and experimentally studied cases that cover a wide range of complex situations presenting a challenging benchmark for the aim of the present work. Our results show that ILS provides a good description of the tunnel topology and a reasonable approximation to the free energy landscape, while MSMD provides more accurate and detailed free energy profile description of each tunnel. Based on these results, a combined strategy is presented for the study of internal ligand migration in heme proteins.

 J Comput Chem 00: 000–000, 2011

Key words: ligand migration; O_2; NO; CO; implicit ligand sampling; multiple steered molecular dynamics; free energy profile; molecular dynamics; proteins; cavities; tunnels; nitrophorin; truncated haemoglobin; xenon sites; docking sites; AMBER; MSMD; ILS; MD

Heme Proteins and Small Ligand Migration

Heme proteins, the family of proteins containing an iron-porphyrin complex as a prosthetic group, are found in all living organisms. They perform a wide variety of tasks such as transport and sensing of gases, electron transport, oxidation of organic compounds, and catalysis of reactions between nitrogen and oxygen reactive species.[1,2] In most cases, subtle regulation of the affinity for small ligands like O_2, CO, NO is the key issue determining a heme protein's function, as shown for different widely studied members of this family, such as hemoglobin and myoglobin[2–5] the NO, O_2, and CO sensors soluble guanylate cyclase,[6,7] Fix-L,[8] and CooA,[9] the Nitrophorins,[10–13] the heme based sensors,[14] and also the newer members of the globin group like the Truncated hemoglobin (trHb) subfamily of proteins,[15–17] Experimentally, the ligand affinity is characterized by the equilibrium constant K_d, determined by the ratio between the kinetic rate constants of association and dissociation (k_{on}/k_{off}), respectively.[1]

Correspondence to: M. A. MARTI. e-mail: marcelo@qi.fcen.uba.ar.
Contract/grant sponsor: Universidad de Buenos Aires; contract/grant numbers: 08-X625, 08-X074, ANPCYT 07-1650, 06-25667
Contract/grant sponsor: Conicet; contract/grant numbers: PIP 01207
Contract/grant sponsor: Guggenheim Foundation
Contract/grant sponsor: EU FP7 program (projects NOstress)

In most heme proteins, ligand association kinetic constant, k_{on}, depends on two processes: ligand migration from the solvent to the heme active site, and ligand coordination to the heme iron.[1] The ligand migration process (first step), is determined by three different factors: the presence of internal cavities and tunnels,[18–20] the presence of specific residues acting as "gates,"[4] and in many cases by the endogenous coordination of residues to iron (internal hexacoordination).[21–24] Iron coordination (the second step) is mainly determined by the spin state of the ligand and the relative in plane position of the iron. For these reasons, in most cases the k_{onO_2} is higher than the k_{onCO}, and k_{onNO} is even higher.[4] Usually, the ligand migration process is dominant, especially when comparing the same ligand in two different proteins. Values of association rates span a range of five orders of magnitude, starting at about 10^4 $M^{-1}s^{-1}$ in those systems with very low accessibility to the iron and rising to 10^9 $M^{-1}s^{-1}$ when the association rate is mainly controlled by the diffusion from the solvent to reach the active site, as observed for isolated porphyrins.[4,25]

On the other hand, the dissociation rate (k_{off}) is also determined by two processes, thermal breaking of the protein-ligand interactions and secondly ligand escape from the active site into the solvent. Dissociation rate constants span a range of roughly seven orders of magnitude, from 10^{-3} s^{-1} to 10^4 s^{-1}.[1,4,26] Different ligands present different diffusion and bond-breaking behavior resulting in different ligand affinities. Oxygen binds exclusively to ferrous (Fe_{II}) heme, and its dissociation rate constant is mainly determined by the interactions between the coordinated O_2 and the interaction with the protein matrix.[27] For CO and NO, dissociation from ferrous heme is mostly dominated by Fe-L bond breaking, and similarly low values ($\approx 1 \times 10^{-2}$ s^{-1}) are observed for many different proteins.[1] An interesting case, however, is presented by the Nitrophorins which bind and release NO from the ferric enzyme depending on the environment pH. They store NO at pH below 6, while releasing it a pH of 7. Interestingly the heme in the ferric form binds NO weakly at both pHs, therefore the NO release is controlled by ligand migration from the distal cavity to the solvent. This example clearly shows that ligand migration, and the presence of tunnels can control not only ligand association, as mentioned above, but also ligand dissociation.[10,11,28,29]

Theoretical and Experimental Methods for the Study of Ligand Migration

Determining the ligand association and dissociation constants for wt and mutant proteins, combined with available structural data for the protein, can yield useful insights into the role of the cavities or tunnels in the ligand migration process.[4,26,30–32] However, understanding microscopic details, and evaluating the dynamics of the system requires microscopic tools capable of probing molecular structure with the ligands inside the protein.

Computer simulation methods, such as molecular dynamics (MD), provide an effective tool for the investigation of protein cavities and the associated ligand migration mechanism cause they provide a combined atomistic detailed structural and thermodynamic picture of the process, that includes the effects of protein motions.[27,33–36] Moreover, although standard molecular dynamics at the nanosecond time scale is not able to provide a complete picture of the ligand migration process, and very long simulations must be performed to allow the ligand to sample the tunnel/cavity system,[37–41] this difficulty can be overcome by the use of different strategies that enhance sampling at an affordable computational cost. Accordingly, several schemes have been developed to study the small ligand migration process in the last decade, as recently reviewed by Arroyo-Mañez et al.[42] These methods are based on the use of different approaches: such as the use of guiding potentials, or simulation at different temperatures for the protein and the ligand,[43] use of a hierarchical optimization approach,[44] the use of grids,[45] or also previously computed MD trajectory, as further explained below.[38,46–49]

A very powerful method to model activated processes such as ligand migration through the protein matrix, is achieved by means of multiple steering molecular dynamics (MSMD) schemes. This technique is especially suited to calculate free energy barriers along the tunnels and has been successfully applied in many cases.[18–20,10,29] In practice, several different MD simulations are performed, where the ligand is pushed from the proteins active site towards the solvent (or pulled inside from the solvent) by means of an external guiding potential. For each steered molecular dynamics simulation (SMD) the irreversible work performed by the guiding potential is measured along the ligand migration path. The free energy is obtained by computing the exponential average of the work values as described by Jarzynski's equality (See the Methods section for details).[50] This methodology has shown, in several works, to display similar performance (in terms of accuracy of the resulting profile) and efficiency (in terms of computational cost) as the more traditional umbrella sampling method[51,52] which has also been used to compute the ligand migration free energy profile in proteins.[53] Finally, also recently, another powerful method called metadynamics[54] was developed to compute free energy profiles, and successfully used to study small ligand migration process in heme proteins.[41,55] These methods have in common a large computational cost, but allow computing free energy barriers for small ligand entry and exit that can be directly compared with the experimental determined rates, showing very good agreement, specially when wt and mutant proteins are compared.[19,20] These methods share also the property of treating the ligand explicitly along the simulation therefore accounting for ligand protein interactions during the process itself.

More recently, another approach, for computing the probability of finding a ligand molecule inside the protein matrix was developed and used to study ligand migration in several globins. This new method uses a series of snapshots taken from previously obtained standard MD simulations of the protein, performed in the absence of the ligand. The method is fast and allows post processing of a previously obtained trajectory, and since the ligand interaction is incorporated only as a probe afterwards, it was called implicit ligand sampling (ILS) methods.[47,48] The ILS method is able to present a complete view of the protein tunnel/cavity system, and was shown to successfully identify several ligand migration channels in Mb, in agreement with the experimentally determined Xenon site and the ligand binding studies of Mb mutants. Clearly, the main approximation per-

formed by the ILS methods is that the explicit presence of the ligand does not affect the local and/or global protein dynamics significantly. Interestingly, the method also provides a potentially very fast determination of the free energy landscape for the corresponding ligand position across the whole protein matrix, using information from a previous MD simulation which was not necessarily designed for the purpose of ligand migration studies.

Given the recent widespread use of ILS method to study cavities in heme proteins, and the lack of a systematic study of its free energy calculations accuracy and correlation with experimental data or comparison with traditional free energy methods, we decided to compare the results obtained with ILS and MSMD methodologies for the identification and characterization of ligand migration free energy profiles across protein tunnels, for a set of selected heme proteins. Secondly, and based on the analysis of the corresponding results accuracy and computational cost, we aim to propose an efficient combined protocol for studying the process.

Specifically, we have selected the intensively studied *Mycobacterium tuberculosis* truncated hemoglobins N (Mt-trHbN) and O (Mt-trHbO), which display a conserved tunnel cavity system which is dynamically regulated by gates residues,[18–20,23,24,56] and the above mentioned NP4 which allosterically regulates NO escape by an open-close mechanism.[10,28,29] The examples cover an experimentally well characterized wide range of complex situations such as ligand entry/escape, dynamical and allosteric control of tunnel opening, and systematic selected mutation studies that alter the tunnel barrier, therefore presenting a challenging benchmark for the aim of the present work.

Computational Methods

Multiple Steered Molecular Dynamics

In the MSMD method the original potential is modified by the addition of a new term $V_{\text{add}}(t)$, which is time-dependent eq. (1) and is set to drive the system through an arbitrary reaction path. When applied to ligand migration, the aim of the potential is to guide the ligand along the tunnel/cavity system allowing overcoming the possible entry/exit barriers.

$$V_{\text{add}}(t) = (1/2)k[x - x_0(t)]^2 \tag{1}$$

In eq. (1) k is an arbitrary constant, x is the actual reaction coordinate (RC), usually describing the ligand motion along the tunnel, and $x_0(t)$ is the time-dependent restrain expressed as a moving equilibrium value of the RC, as described by eq. (2).

$$x_0 = x_i + vt \tag{2}$$

Where t is the time-step of the MD simulation, and v is the speed at which the RC, and therefore the ligand is guided. As shown in several works v is the key parameter when doing MSMD. In the case of small ligand migration through internal tunnels of proteins presented here, the chosen RC is the distance between the ligand and the active site heme iron atom.

Using this methodology, the external (nonequilibrium) work (W) necessary to guide the system (i.e., the ligand) along the chosen RC can be computed by integrating over the external force. Starting from different initial configurations many different nonequilibrium works are computed, for the same reaction path and using the Jarzynski's equation [eq. (3)], which relates these irreversible works with free energy changes; it is possible to obtain the free energy of the process.

$$e^{-DG/kBT} = \langle e^{-W/kBT} \rangle \tag{3}$$

In eq. (3) k_B is the Boltzmann constant, T is the temperature, and W is the calculated work for each independent nonequilibrium process.[50,57] The term MSMD is applied since multiple MD simulations of the process are needed to obtain accurate free energy profiles. In all simulations the ligand is explicitly considered.

Is must be pointed out that this methodology is not only applicable to computational studies. In fact, many experimental and mixed theoretical/experimental works have been done where out-of-equilibrium information is used to estimate free energy profiles.[58,59] In the work done by Hummer and Szabo[58] the authors show how free energy surfaces are reconstructed rigorously by repeated pulling experiments and Jarzynski's equation. Mills and Andricioael[59] showed how experimental data can be used to derive free energy profiles which are in turn used for optimal restraining potentials that guide simulation along relevant pathways, decreasing overall computational time.

ILS Method

The ILS approach is based in the calculation of the potential of mean force (PMF) corresponding to the placement of a small ligand inside each region of the whole protein matrix. The corresponding PMF is associated to the free energy cost of incorporating the ligand at each particular position and therefore describes which regions of the protein are accessible to the ligand and to what gain/cost. The methodology relies on the fact that small ligands are, obviously, small and interact weakly with the protein matrix and therefore the interaction can be computed for protein structures that were obtained without the presence of the ligand in previous MD simulations. By performing the SMD of the protein without the ligand and treating its presence as a weak perturbation added afterwards, sampling of the ligand can be performed on the whole protein matrix simultaneously, from just one sufficiently long plain MD simulation.

The PMF of the ligand or the Gibbs free energy of the ligand at point r in this case, $G(r)$, can be associated directly with the probability of finding the ligand at position "r," which from a previous MD simulation according to eq. (4):

$$G_{\text{ILS}}(r) = -k_B T \ln \sum_{n=1}^{N} \sum_{k=1}^{C} \frac{e^{-\Delta E_{n,k}(r)/k_B T}}{NC} \tag{4}$$

Where the summation is performed over M MD snapshots, and C randomly chosen ligand orientations, and the $\Delta E(q,r)$ is the protein ligand interaction energy, with the ligand at position "r" and the protein conformation is represented by "q," and

consist solely of a Lennard-Jones interaction. In practice, the computation of the PMF is carried out over a regularly spaced grid of possible ligand coordinates "*r*." More details can be found in the corresponding original works.[48]

In the present work ILS free energy profiles are computed using 10–50 ns long MD simulations, using 100, 1000, 5000, or 10,000 snapshots and grid spacing of 0.5 to 2Å as described for each case. The ILS calculation were performed with the VMD plugin.[48]

Set up of the Systems and Simulation Parameters

All initial structures for the MD simulations were taken from the corresponding crystal structures, or *in silico* built mutants as described in the corresponding works. MD simulations where performed in explicit octahedral box of TIP3P water at 1 atm and 300 K, maintained with the Berendsen barostat and thermostat, using periodic boundary conditions and Ewald sums (grid spacing of 1 Å) for treating long range electrostatic interactions. The SHAKE algorithm was used to keep bonds involving H atoms at their equilibrium length and a 2 fs time step for the integration of Newton's equations. For all cases we used the Amber ff99SB force field parameters for all residues,[60,61] except the heme where we used our own thoroughly tested parameters.[27] All simulations where performed with the SANDER module of the AMBER9 program package.[60,61]

As mentioned above the free energy profiles computed with the MSMD method were obtained by performing several ligand pulling/pushing experiments and combining the resulting work vs. RC profiles using Jarzynski's equation. For TrHbN the free energy profiles were constructed using pulling speeds of 0.05 and 0.1 Å/ps, which yielded similar profile, and a force constant of 200 kcal/mol.Å. The profiles corresponding to long and short tunnels were built combining smaller segments which were computed each using 10 MSMD simulations (each 1 ns or 2 ns long) starting either at the distal cavity, the four crystallographic Xenon binding sites and the tunnel entrance. Simulations were typically performed for each of the two pulling velocities. In cases in which two overlapping profiles were obtained (from entry and exit sets), we confirmed that both of them matched. The total amount of MSMD simulation was of ca 500 ns. For TrHbO the profiles were computed using a 0.1 Å/ps pulling speed and a force constant of 200 kcal/mol A. For each profile two blocks of 10 MSMD were performed. Each 1 ns long MSMD was started from a snaphsot taken from an equilibrated MD run with the ligand at fixed distance from the iron at the tunnel entry or inside the located minima along the tunnel, just before the measured barrier. These simulation correspond to a total of 120 ns MSMD simulation time. For Nitrophorin 4, the NO escape free energy profiles were computed from 20, 1 ns long MSMD simulations, starting from equilibrated structures of the NO bound protein in the open and closed states respectivly. Profiles were computed using a 0.1 Å/ps pulling speed and a force constant of 200 kcal/mol Å, corresponding to a total of 40 ns time of MSMD simulation.

Results

Tunnel Cavity System in Mt-trHbN

Mt-trHbN is one of the most studied heme proteins concerning its ligand binding characteristics and tunnel cavity system. High Xenon pressure crystallographic studies,[30] showed that Mt-trHbN hosts two potential perpendicular tunnels, called long tunnel (LT) and short tunnel G8 (STG8) that connect the heme active site with the solvent. The protein structure is shown in Figure 1E. We start with this system to analyze ILS performance. For this sake we performed an analysis of the number of snapshots needed to have meaningful results with ILS. Based on a 100 ns long MD simulation, we selected different number of snapshots and computed the corresponding ILS isosurfaces. For all cases the same simulation time interval was selected, spacing the selected snapshots for ILS calculations using different time intervals to collect the desired amount of snapshots. As shown in Figure 1A (100 snapshots used) significant ligand finding probability (LFP) is already found along both tunnels. When we used 1000 snapshots, the tunnels are now clear and well connected with the distal pocket (DP). Using 5000 snapshots makes only minor changes in tunnel topology (mostly a smoothing of the isosurface boundaries) and no improvement is observed by using 10,000 snapshots. The results are consistent with the experimental Xenon X-ray data[30,62] and with previous studies from our group using explicit ligand MD simulations[18,24]

Another interesting fact on Mt-TrHB long tunnel is that the crystal structure[30] and also previous theoretical works,[18,24] have demonstrated that PheE15 can act as a gate residue blocking the LT, and that this gate is dynamically regulated by the coordination state of the heme-group. In the deoxygenated protein PheE15 is blocking the tunnel, making ligand entry more likely to occur through the short tunnel. In the oxygenated state the PheE15 gate enters in a dynamical equilibrium that opens the long tunnel (LT) transiently during several nanoseconds, allowing efficient ligand migration through it.[18,24] In LT of Mt-trHbN, there are three cavities or energy wells (also called secondary docking sites, denoted S1, S2, and S3) that correspond to the location of the Xenon sites obtained by X-ray crystallography.[30–32] The first one is located at about 18Å from the heme, after the tunnel entrance, the second can only be identified in the PheE15 closed state, just before the Phe ring at about 13 Å, and the third is revealed when the PheE15 moves to the open state at about 11 Å, just before the distal cavity holding the oxygenated heme.

Based on the above observations we decided to test whether ILS analysis is able to detect the PheE15 gate dynamics in the oxy state. We computed the ILS surface for selected time intervals with PheE15 in either the open or closed configuration. Based on the ILS surface we computed for each case the free energy profile along the LT from the solvent till the heme active site. The results are shown in Figure 2A, together with the free energy profiles for explicit NO migration in the open and closed states (Fig. 2B) as computed with MSMD in our previous work.[18,24] As shown in Figure 2, both methods present similar results. The shape of the profiles and the number and location of the minima and maxima are similar using both methods. For the closed state (dotted line) two wells corresponding to Xe sites 1 and 2, are clearly observed (specially the second one), while in the open state the second site disappears and the Xe site 3 is found.

The main differences between both profiles are in the 14–18 Å range, which could not be computed separately for the open

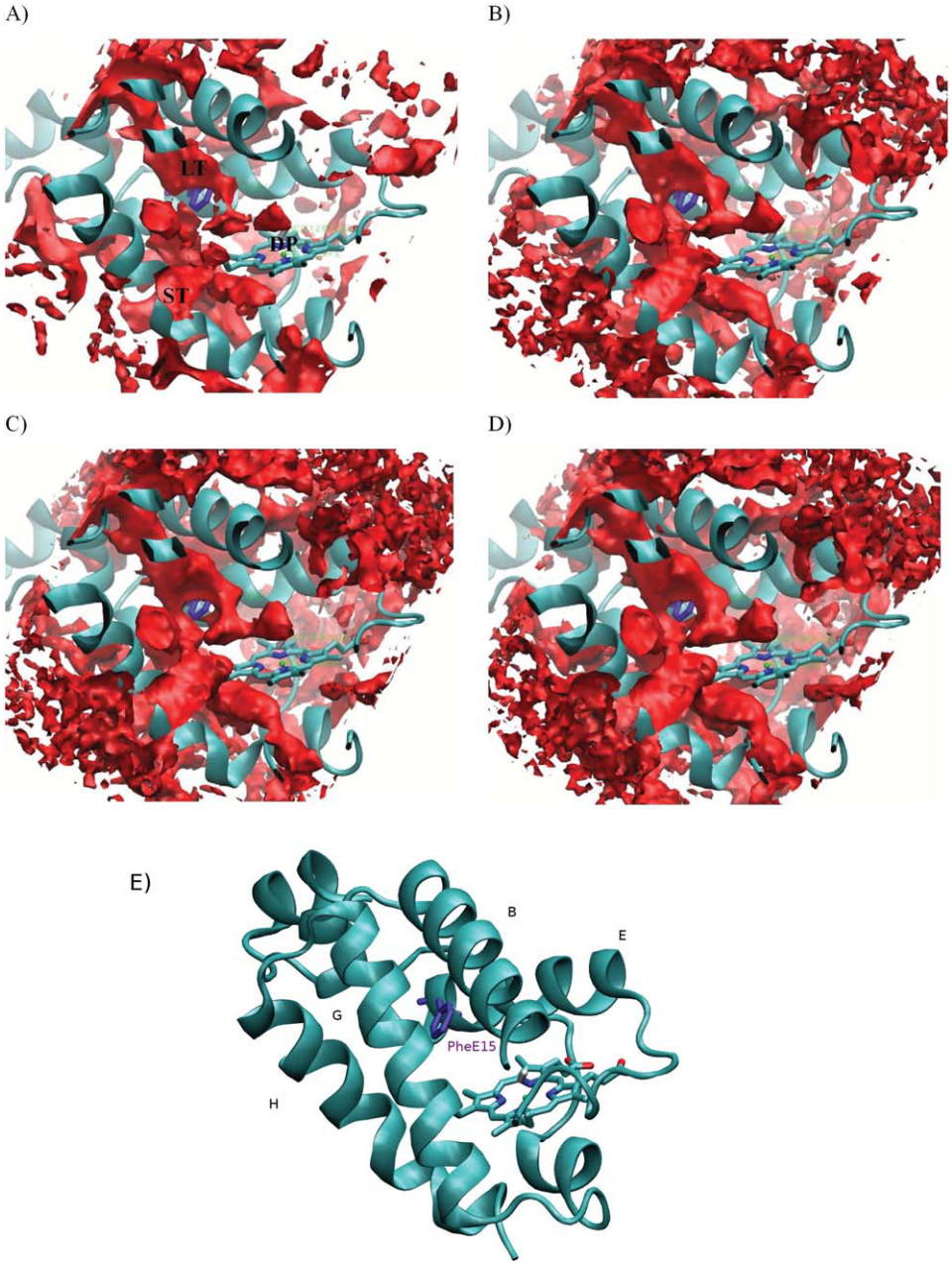

Figure 1. Mt-TrHbN tunnel/cavity system (red) determined using the ILS method with a grid resolution of 0.5 Å, and using: (A) 100 snapshots (upper left), (B) 1000 snapshots (upper right) (C) 5000 snapshots (lower left), and (D) 10,000 snapshots (lower right). Heme (cyan) and Phe15 (violet) are shown as sticks representation in violet. ST: short tunnel, LT: long tunnel DP: distal pocket. (E) Mt-TrHbN protein structure.

and closed LT cases using MSMD and therefore represents an average of both states. This was done due to the fact that when the ligand is located in this region, the Phe-E15 gate may open or close in the timescale of the simulation, not allowing the proper assignment to a given state. The results, however, show that with the MSMD method a small barrier separates Xe site 1 from Xe site 2 (or Xe site 3), while the ILS method shows for the closed state a small barrier going form Xe site 1 to Xe site 2, but a bigger barrier for the reverse process. In the open state the barrier form Xe site 1 to now Xe site 3 is slightly larger compared with that obtained with MSMD.

Concerning the effective barrier for migration towards the heme, the MSMD method predicts a barrier of about 4–5 kcal/mol in the closed state, that is reduced to less than 2 in the open

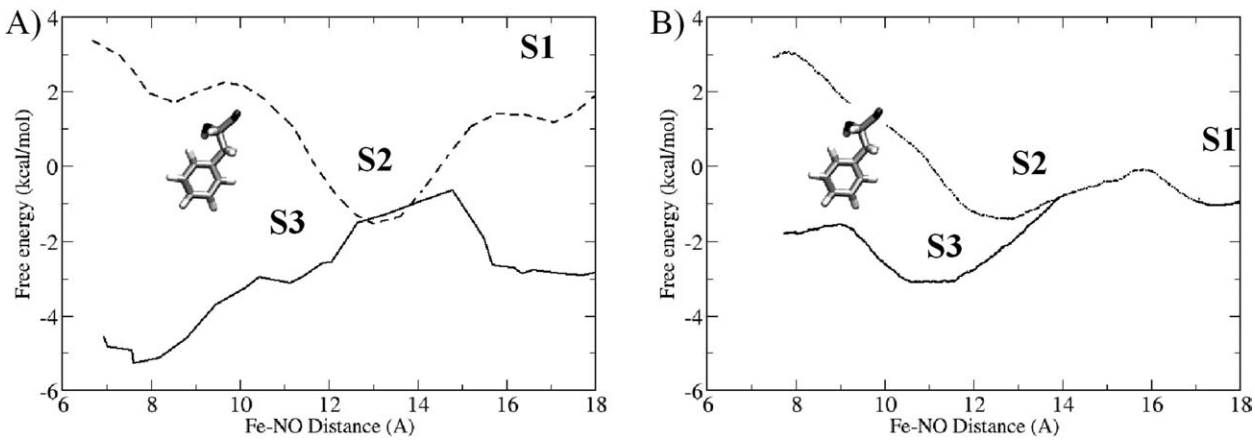

Figure 2. Free energy profile along Mt-trHbN long tunnel for the open (solid line) and the closed (dotted line) conformation of PheE15. (A) Using ILS. Grid resolution of 0.5Å (B) Using MSMD.

state. ILS method shows for the closed state an effective barrier of also about 5 kcal/mol that is reduced to almost 0 kcal/mol in the open state. Clearly, both methods are able to distinguish both states and yield significant different tunnel topologies and barriers.

We now analyze if the number of snapshots or the grid resolution used for the calculation affects the quality of the free energy profile computed with the ILS method. We computed the LT profile shown above for the closed Phe-E15 state, using different number of snapshots (Fig. 3A) or a different grid resolution (Fig. 3B).

As shown in Figure 3A, with only 100 snapshots the profile is very noisy, and only with over 1000 snapshots a reasonable smooth profile is obtained, which only gets slightly better with an increasing number of frames. No difference is observed between 5000 and 10,000 snapshots. These results show the same trend as those shown above for the tunnel topology. Figure 3B shows the effect of grid resolution on the profile convergence; highlighting that a 2 Å of grid resolution is insufficient to have an accurate profile. On the other hand, a smooth profile is already obtained with 1 Å resolution, and only a minor improvement is observed when the resolution is reduced to 0.5 Å. Using a better resolution makes no sense since it is already less than half size of the probe. In summary, good quality free energy profiles are obtained with the ILS method using between 1000–5000 snapshots and 0.5–1 Å resolution. For that reason the following computed profiles are obtained using 10,000 snapshot and 0.5 Å grid resolution.

For the sake of completeness of the tunnels in Mt-trHbN, the free energy profile for O_2 migration along the short tunnel (STG8) in the oxygenated and deoxygenated proteins was also computed using ILS methods and presented in Figure 4, together with the MSMD results. The shape of the profiles present some differences, since the minima and maxima are located in differ-

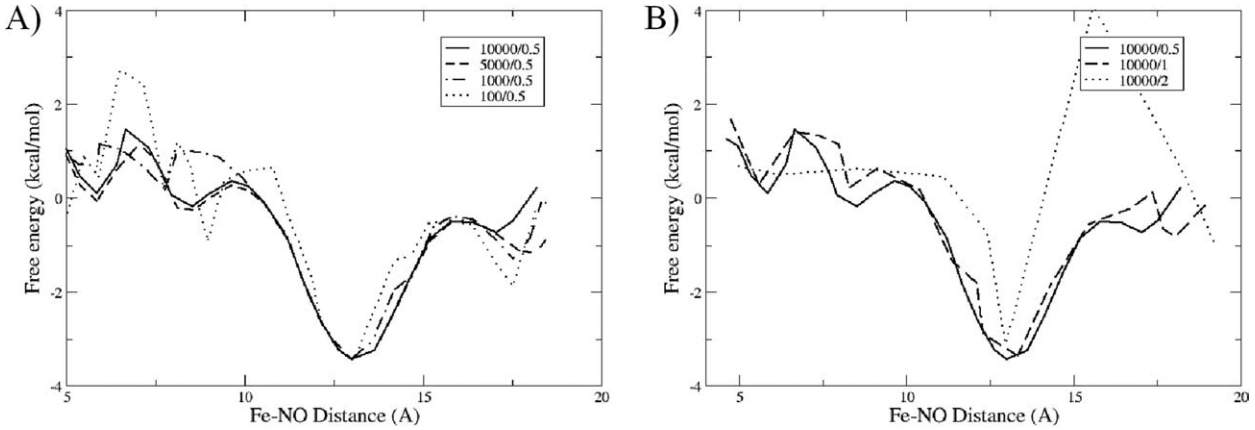

Figure 3. ILS Free energy profiles for NO migration along the Mt-trHbN long tunnel in the closed state, using a grid resolution of 0.5 Å. (A) Effect of the number of snapshots: 100 (dotted), 1000 (dotted-dashed), 5000 snapshots (dashed) and 10,000 (solid). (B) Effect of the grid resolution: 2 Å (dotted), 1 Å (dashed), 0.5 Å (solid), using 10,000 snapshots in each case.

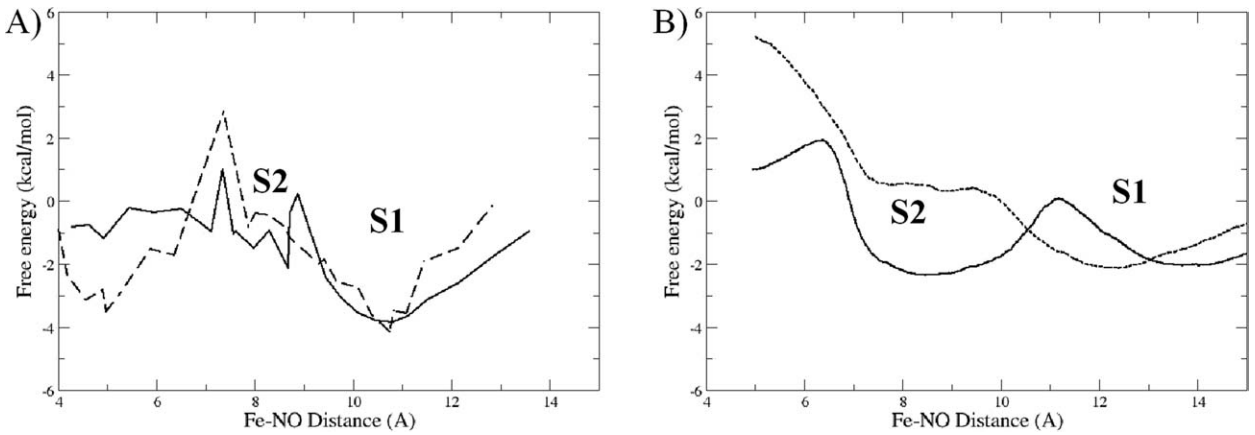

Figure 4. ILS (left) and MSMD (right) free energy profiles for O_2 migration along the TrHbN short tunnel in the Oxy (dashed) and Deoxy (solid) states. Parameters for ILS are: 10,000 snapshots and grid resolution of 0.5 Å.

ent positions. However the order of magnitude of the barriers is similar with both methods. Specifically, the first secondary docking site is clearly identified at about 11Å with the ILS method in both oxy/deoxy states which corresponds to S1 obtained with the MSMD method, although in this case the site is shifted further from the heme, especially in the deoxy state. In the deoxy state, a second site S2 is predicted by both methods at 8 Å, which disappears in the oxy state as also evidenced with both methods. Finally, ILS predicts 7, and 5 kcal/mol barriers for the oxy and deoxy states, respectively, while the barriers obtained with MSMD are of 7, and 4 kcal/mol, respectively. The barrier in the deoxy state computed with ILS is however quite noisy.

A final important point concerning above described results for both methods is how they relate to available experimental data. Concerning tunnel topology, the comparison as already mentioned is striking. Both methods predict the presence of the experimentally determined Xenon sites,[32] with great accuracy. The only drawback seems to be the possible additional paths or tunnel identified by ILS which lack experimental correlation. Concerning the barriers experimental kinetic data for MtTrHbN shows that NO entry to the oxygenated protein, is 30 times faster than oxygen entry to the unligated heme, with values of 745 and 25 uMs^{-1}, respectively. Also, CO recombination data showed the existence of different ligand-dependent conformations, which were later assigned to the PheE15 open and closed states.[18,26,63,64] The MSMD results analysed together for both tunnels provide as described in our previous work a reasonable explanation for this difference, which relies on the opening of the long tunnel (which becomes almost barrierless), and the slight increase in the short tunnel barrier for ligand entry in the oxygentaed protein.[18,24] The ILS method also less accurate seems to also reproduce this trend.

Comparative Ligand Migration Profiles in wt Mt-trHbO and Site Directed Mutants

Similar to Mt-trHbN, the other truncated hemoglobin of M. tuberculosis (Mt-trHbO) displays two tunnels connecting the heme active site with the solvent. The LT which is topologically equivalent to that found in Mt-trHbN, and a short tunnel called STE7. In this group of proteins, the STG8 is not present because there is a Trp in position G8 blocking the corresponding tunnel. The protein structure is depicted in Figure 5B. Different experimental and computational mutagenesis studies revealed that in this protein the LT partially controls ligand entry whose size is regulated by the nature of both TrpG8 and LeuE11.[19,44,56]

To analyze if the ILS method is capable of correctly predicting the trends in the ligand migration barrier for wt and TrpG8Phe and TrpG8Ala mutants of Mt-trHbO, we computed the corresponding free energy profiles for the wt and mutant proteins, from 50 ns long MD simulations for each protein. Similar to the results observed for Mt-trHbN, the ILS method correctly predicts the topology of the LT, passing next to TrpG8 as shown in Figure 5A. The results for the resulting free energy profiles for wt, TrpG8-Phe and TrpG8-Ala mutants obtained with ILS are shown in Figure 5C, and those obtained with MSMD in Figure 5D.

The MSMD results show that the Mt-trHbO long tunnel (LT) displays a large 6 Å wide cavity centred at 10 Å from the heme, oxygen is drawn to this big hydrophobic cavity from the solvent as showed in the gain of 2–4 kcal/mol in free energy along the process (Fig. 5C). To migrate from the cavity to the heme and bind to the iron oxygen must overcome a large 12 kcal/mol barrier due to the hindrance of the conserved TrpG8 and LeuE11 residues. The barrier is reduced to 5 kcal/mol in the TrpG8-Phe mutant and to only 2 kcal/mol in the TrpG8-Ala mutant (Fig. 5C). Consistently, the observed association rates increases with the corresponding mutations, as observed by Guallar's group.[44]

The ILS profile obtained for wt Mt-trHbO fails to predict the gain in free energy when the oxygen moves from the solvent to the large cavity (Fig. 5B). Only the TrpG8-Phe mutant predicts this gain in energy correctly. The failure to completely predict this gain in energy when the oxygen moves from the water solvent towards the hydrophobic cavity tunnel probably arises due to sampling issues, since it is very difficult to reach a uniform correct value for the free energy of the probe in the explicit sol-

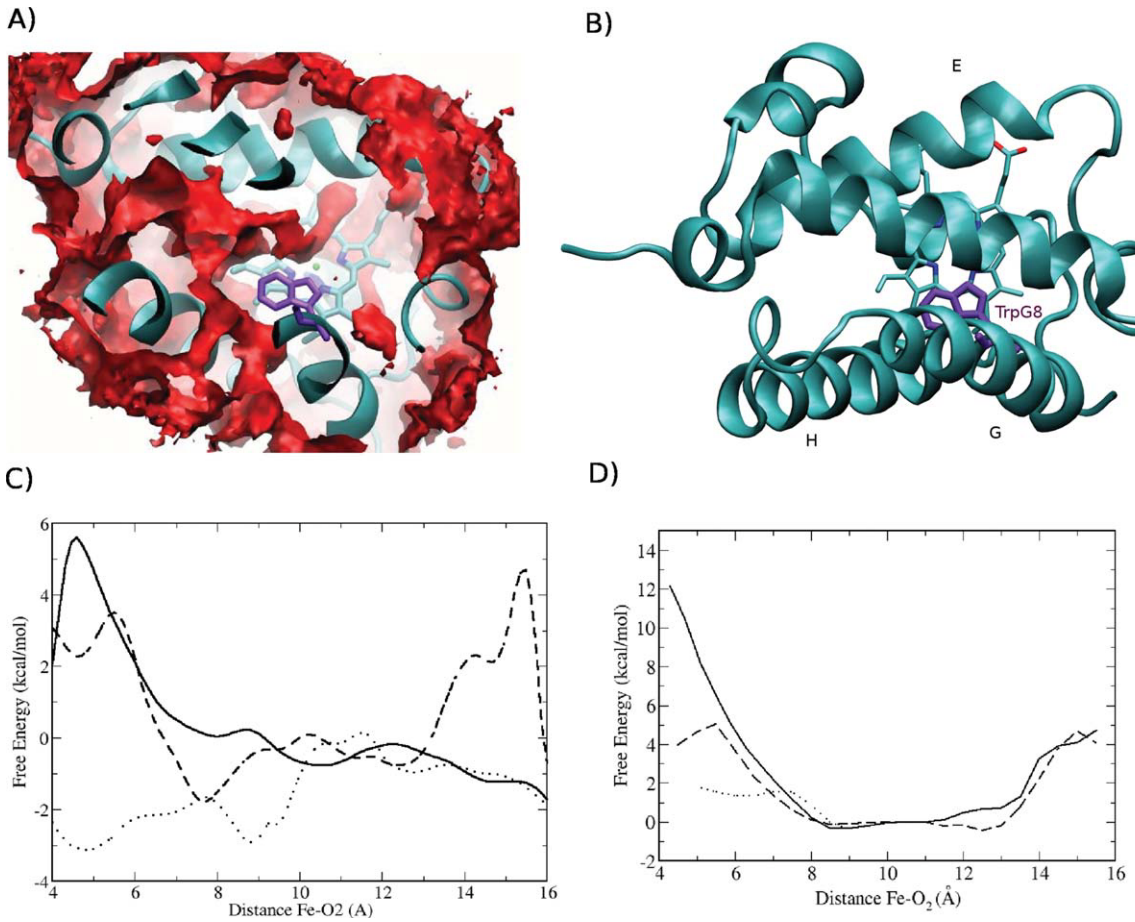

Figure 5. (A) Mt-trHbO long tunnel computed with ILS, showing the presence of TrpG8 (violet sticks). (B) Mt-trHbO protein structure. (C) Free energy profile for ligand migration in wt protein (Solid line) TrpG8Phe (dashed line) and TrpG8Ala (dotted line) mutants computed using the ILS method. (D) Free energy profile for ligand migration in wt Mt-trHbO (Solid line) TrpG8Phe (dashed line) and TrpG8Ala (dotted line) mutants computed using MSMD method.

vent using ILS. Concerning the barrier to reach the heme, ILS correctly predicts the trend in mutant proteins, showing a significant decrease in the barrier for TrpG8-Ala. However, in contrast to the MSMD method, for the TrpG8-Phe and wt ILS predicts similar (but smaller) barriers and only a minor decrease for TrpG8-Phe the mutant.

Prediction of the Open and Closed States for NO Escape in NP4

The final case to be tested is that of nitrophorin 4 (NP4). Previous studies from our group showed that NP4 exists in two different pH dependent states which control NO release from the heme active site towards the solvent by modulating the free energy barrier of ligand escape. Based on previous experimental observation we showed that stable MD of each state, closed/low-pH and open/high-pH can be performed by selecting the corresponding appropriate initial X-ray structure and setting a differential protonation state for the key residue Asp30. To analyze whether the ILS method is able to topologically describe the NO release path, we performed 50 ns long MD simulations of protein in each state and computed the corresponding ILS isosurface as shown in Figures 6A and 6B for each case. For comparative purposes Figure 6C shows the NO escape path form the open conformation determined using plain NO free MD simulations, and also NO migration further inside the NP4 protein in the low pH closed state.[10]

For comparative purposes Figure 6C shows the NO escape path from the open conformation determined using plain NO free MD simulations, and also NO migration further inside the NP4 protein in the low pH closed state.[10] The plain direct MD simulations were performed starting from the equilibrated NO bound structures in both states and removing the Fe-N bond from the force filed. For each case (low and high pH) three independent simulation were performed. In the high pH state NO always escapes at simulation times of 1, 5, and 7 ns. While for the closed

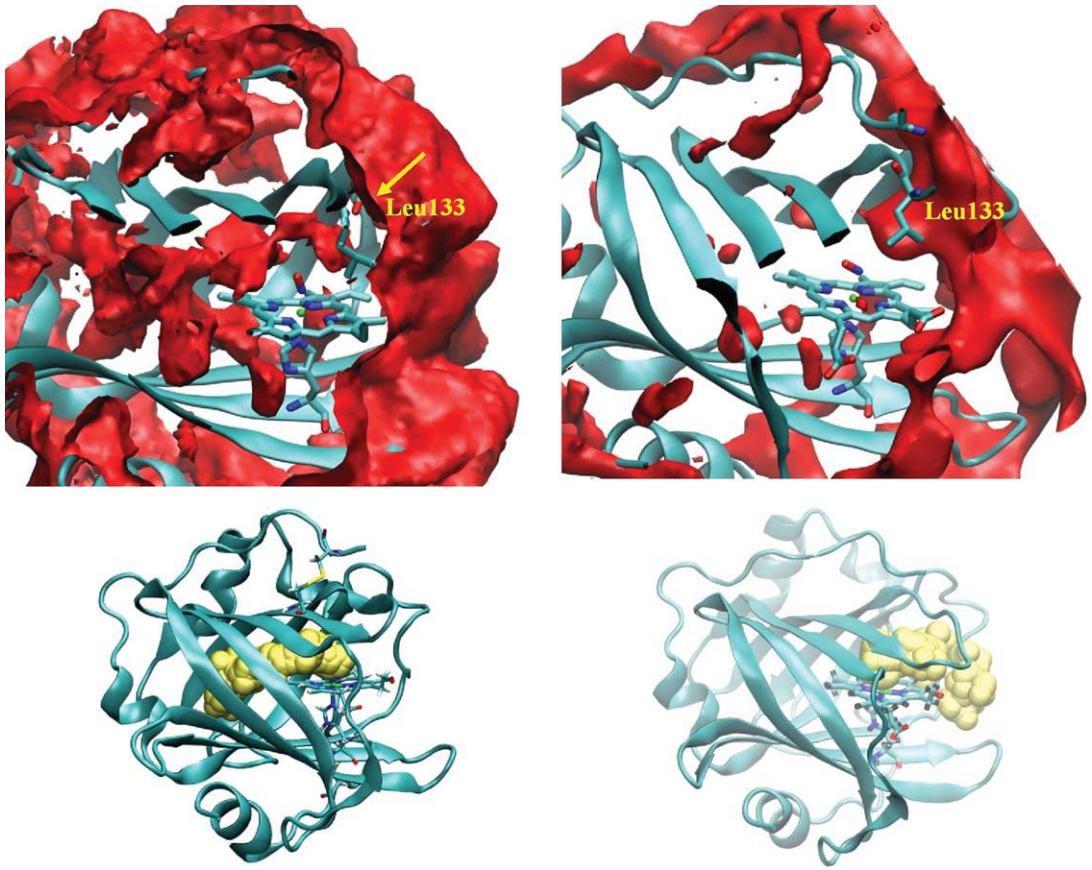

Figure 6. Upper panel NP4 ILS isosurfaces computed along the low pH simulation/closed state (Upper-left panel) and high pH simulation/open state (Upper-right panel, 2 kcal/mol). 10,000 snapshots, Grid resolution is 0.5 Ang. The NO migration path for the low pH state (Lower-left panel) and NO escape path for the high pH state (Lower-right panel). [Color figure can be viewed in the online issue, which is available at wileyonlinelibrary.com.]

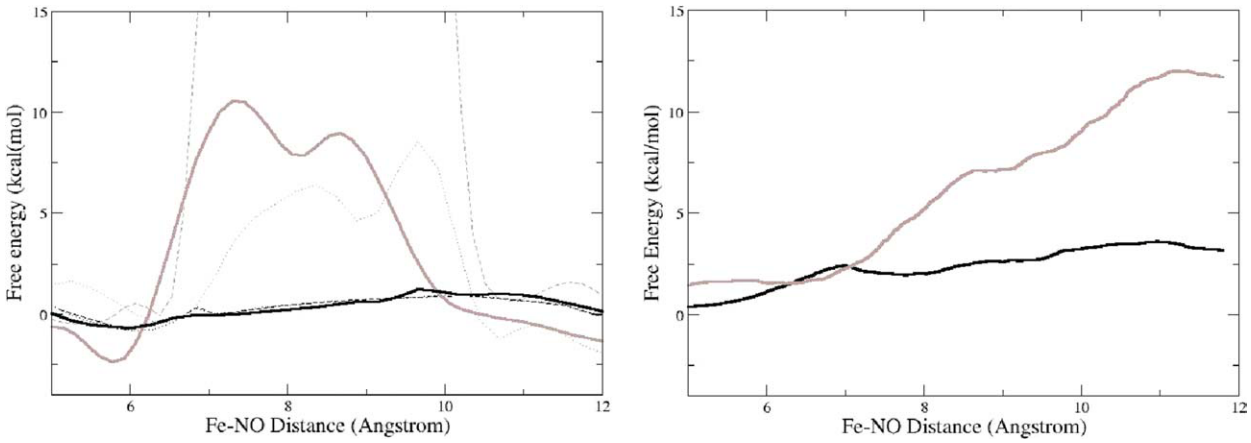

Figure 7. Free energy profile for NO escape in NP4 low-pH (gray line) and high-pH (black line) using ILS (left panel) and MSMD (right panel) method. For ILS the following time intervals were considered: 10–30 ns (dotted), 31–50 ns (dashed), and 10–50 ns (solid) time intervals were used. [Color figure can be viewed in the online issue, which is available at wileyonlinelibrary.com.]

state the NO remains inside the protein in all three cases and moves further inside the protein up to 20 ns simulation time.

Figure 6 shows that ILS method correctly predicts that ligand escape path is closed in the low pH conformation. Indeed, there is no continuous path between the protein DP and the external solvent, even using a 5 kcal/mol value for drawing the surface. The path is clearly blocked by Leu133 shown by the yellow arrow (Fig. 6 Upper-left) and consistently with previous MD results. Also consistent with the results in the closed state, the NO prefers migrating further inside the protein (compare upper and lower left panels). In the high pH state, on the other hand, there is a clear connection between the DP and the solvent (evident already at 2 kcal/mol drawn isosurface), which passes next to Leu133 which has moved due to the NP4 conformational change. The ILS predicted NO escape path is very similar to the actual path described by the explicit NO molecule shown in Figure 6 lower right panel.

Although the results presented above show that ILS method can qualitatively distinguish NP open and closed states, we now analyze if ILS is capable of predicting the free energy difference for NO escape. For this sake we computed the corresponding profile using ILS for different time intervals along the simulation. The results together with those obtained with MSMD in our previous work are shown in Figure 7.

The results in Figure 7 show that ILS is able to capture the difference in the NO escape profile between the low pH (gray lines) and high pH (black lines) conformations qualitatively (Fig. 7 left panel). Strikingly, for the high pH open conformation the profiles and barriers obtained with ILS for any of the selected time intervals is very similar to the one obtained with MSMD. For the closed low pH state, however the shape of the profile and the minimum location are different. In this case, the barrier value and profile topology obtained with ILS are strongly dependent on the amount of simulated time and the chosen time interval, although for all cases a significant higher barrier as that compared with the open state is obtained. An interesting case is presented for the low pH profile computed with ILS for the 31–50 ns time interval which shows a barrier of about 50 kcal/mol (not shown) probably reflecting that during this time the path remained completely blocked. An interesting possibility therefore, is that for partially blocked tunnels with high barriers (like that of NP4 in the closed state) the presence of the ligand itself, as in MSMD, induces the presence of a narrow path. In its absence (as in ILS) the path is completely blocked and unreasonable high barriers are obtained.

As for the previous cases, the obtained results can also be directly compared with the available experimental data. Concerning the predicted NO escape path, there is no available data. However, high pressure Xenon crystallography of NP4 at low pH shows the presence of a Xe site close to the proximal site which coincides with the path followed by the NO in the closed state observed in the MSMD and free NO simulation data. Finally, and consistent with a significant change in the NO escape barrier, reported values for the NO release rate show a 50 times increase when the pH is changed from 5.0 to 7.5.[11]

Discussion

As mentioned in the introduction, the aim of this work is to compare the performance of ILS and MSMD methods for the study of small ligand migration, and based on the preceding analysis of the results accuracy and computational cost propose an efficient combined protocol that allows straight forward determination of free energy profiles for small ligand migration across the protein matrix. For this sake, we have selected three examples whose ligand migration mechanism are well characterized experimentally,[11,26,44,65] which had been thoroughly studied using MSMD methodology in our group,[10,18,19,24] and shown to be in excellent agreement with the available experimental structural, spectroscopic and kinetic data.[11,26,44,65] By analysing the corresponding cases with the ILS method in several ways, we were able to determine the computational cost needed to obtain good and accurate results, and also the method limitations and drawbacks. The conclusions of the preceding analysis for different aspects of the small ligand migration process are presented below.

Comparison of Computational Cost

To analyze the efficiency of both methods, we start by briefly reviewing the technical issues (directly related to the computational cost) concerning the MSMD method accuracy. To obtain accurate free energy profiles (in good agreement with experimental observations) with MSMD, three issues have to be considered. First, adequate sampling of the protein conformational space is needed. Secondly, proper selection of the pulling/pushing speed, and third a good number of SMD simulations, that ensure convergence of the profile with reasonable statistical error. Protein conformational sampling, is of course case dependent, but based on our experience, for those proteins where the ligand migration path is stable and no significant conformational changes occur, such as Mt-trHbO and NP about 20–30 ns of plain MD are required. However, it is recommended to use longer dynamics analysis different segments of the trajectory to detect possible changes in the profile. For cases in which conformational changes are involved, such as Mt-trHbN LT, longer simulation times are needed and a careful analysis of the profiles obtained during different simulation segments is recommended. Pulling speed is a difficult parameter to estimate from scratch but based on our experience 0.005–0.01 Å/ps are slow enough to obtain profiles of small ligand migration across protein tunnels. This results in the need of simulating 1–2 ns for a 10 Å long profile. Finally, usually at least 20 different SMD are required to obtain good convergence of the resulting profile, with a statistical error of about 1 kcal/mol. In summary about 20–40 ns explicit ligand MD are needed for each profile using MSMD.

Concerning the ILS method, our results show that the number of frames seems the less sensitive parameter provided enough statistics (1000 snapshots) are used. But considering that a 1 ns long simulation usually hosts this number of frames and that calculations for 1000–5000 frames are fast (30–300 minutes for a 0.5 Å grid resolution, depending on system size) it is not justified to reduce the number. Similarly, grid resolution of 1 Å or better 0.5 Å are sufficient to obtain converged profiles, but more

coarse-grained grid is not recommended. Finally, it should be noted that resulting profile depends on the MD simulation time as any property that requires a proper sampling of the protein conformational ensemble, and the considerations are the same as those mentioned above.

Based on the above described data the computational cost for both methods can thus be compared. For a case like Mt-trHbN, the initial simulation time required to adequate sample both conformations is the same for both methods. Once this is done, additional computational cost of ILS is very low, since all needed snapshots are available, and computing the 2 or 3 profiles (using 5000 snaps and a 0.5 grid resolution) requires about 12 hours each on a single processor in a quad-core state-of-the-art personal computer. On the other hand, for computing the open and closed LT profiles using MSMD at least additional 40 different (1 to 2ns long) MD simulations of pulling/pushing the ligand are needed, which may need as much as 100 hours each in 1 processor. The same holds for the other cases. In summary after having performed initial MD sampling the additional cost of ILS is negligible when compared to the MSMD additional cost, which is similar to the amount used for the sampling.

Therefore, from the pure computational cost viewpoint it is clear that ILS is the method of choice. The question then arises as to where it yields meaningful results and where does it fail, and how can we take advantage of the ILS results to reduce or improve more costly calculations such as MSMD.

Global Description of the Secondary Docking Sites and Tunnels

The results show that ILS method correctly predicts the topology of the tunnels. Moreover, with ILS (and not with MSMD where each path must be sampled independently), all possible tunnels are obtained with just one calculation. However, the reverse side of this coin may rely on the difficulty for proper tunnel identification, since many possibly non physiologically relevant cavities are also found by the method, and that for some cases (as the NP) it is very difficult to identify and quantify an actual difference unless one already knows where to look. In any case, given its low computational cost it can yield a very useful first picture of the tunnel cavity system of any given protein.

Free Energy Profiles and Barriers

The results presented for Mt-trHbN long and short tunnels, for Mt-trHbO and for the escape path of NP, shows that the free energy profiles computed with ILS, can only be taken as qualitative pictures. Although, most wells (secondary docking sites) are correctly predicted for several cases, and the presence of barriers is evidenced, barrier heights are not accurate enough when using the MSMD profiles as references. The main problem of the ILS methodology seems to be the an underestimation of high barriers as seen for wt Mt-trHbO and high variability and uncertainties for higher barriers as those found in the NP closed state. Dealing with single point mutants that subtly modify the barrier along a selected path, as for Mt-trHbO is also a tough case for ILS. The method, although correctly predicts the trend in the active site access barriers for TrpG8-Ala mutant, has problems when comparing a more conservative mutation, such as TrpG8-Phe, and shows quite big uncertainties and unjustified differences for ligand movement form the solvent towards the tunnel hydrophobic entry. In summary, although ILS may yield a qualitative picture of the free energy profiles along the tunnels it lacks accuracy and detail of more costly methods.

Comparison with Other Methods for Small Ligand Migration Studies

Although, it is not the scope of the present work to exhaustively compare all methods that can be used to study small ligand migration, we will briefly comment on possible alternative strategies as those presented here. A brief review or all available methods and their application examples for ligand migration studies can be found elsewhere.[42] Other alternatives for obtaining the global picture of the tunnel cavity system are GRID-MD,[45] the pathfinder algorithm[38] and locally enhanced sampling (LES).[46,66] Similar to ILS, GRID-MD uses a previously obtained trajectory to compute a boltzmann weighted occupancy grid which is used for computing possible ligand entry/escape paths. Although, the method has been successfully used for determining tunnels in several globins, it does not allow computing any thermodynamic information, (no free energy is associated with the obtained paths) and therefore given the equivalent computational cost, ILS should be used. Concerning the pathfinder algorithm as developed by Ruscio et al.[38] it very similar to the actual ILS, since a previous MD trajectory is used to compute where, in each snapshot, a probe the size of the ligand fails to overlap with any protein atom treated as hard spheres. So instead of an energetic criterion as in ILS, a geometric criteria is used to determine the internal cavities. The method is rather new and has only been successfully applied to Myoglobin, but could be used as an alternative to ILS. However, the main drawback again is that calculation of free energy is not straight forward. Finally, the LES method is possibly the oldest and widely studied method for detection of tunnels and cavities. In LES multiple copies of the ligand (usually about 10) are simulated simultaneously, and their interaction with the protein is averaged. The method is more costly than ILS and does not allow the use of previous MD. Furthermore, no thermodynamic data can be obtained, and the use of an averaged interaction may result in the occurrence non realistic entry/exit paths. In summary, due to its ability to take advantage of a previously computed trajectory, and the determination of the free energy surface associated with the cavities, makes ILS the method of choice for first, fast rough tunnel cavity characterization.

Concerning, the determination of accurate free energy profiles for ligand migration along a given selected tunnel, and the corresponding barrier estimation, any of the methods mentioned in the introduction, MSMD; Umbrella Sampling or Metadynamics will yield similar results and possibly with similar computational cost.

Summary of Proposed Combined Strategy

Based on the previous analysis for the presented cases, it is clear that once a relatively long plain MD was performed to analyze

protein conformational space and dynamics, as is the usual case for these studies. ILS should be used to compute a complete description of the tunnel cavity system of the protein. Once this is done, more accurate comparative free energy barriers estimation should be performed for selected key tunnels with MSMD (or other free energy method such as Umbrella Sampling). Computation of detailed profile with explicit ligand methods also reveal subtle protein ligand interaction dynamics that allow for the identification of important residues for the migration process.

Conclusions

Based on the results and analysis presented in the present study we can conclude that the ILS method provides a fast and good general description of the tunnel topology and, in general, preferred ligand locations inside a protein, and also a first approximation for estimating free energy profiles for ligand migration along the presented tunnels, and should be the method of choice for initial characterization. The main difficulty with ILS seems to be the accurate prediction of barriers, especially higher ones which are either underestimated or difficult to converge. For accurate and detailed free energy calculations, MSMD presents an ideal partner to ILS, although also other free energy methods such as umbrella sampling or metadynamics may be used. In summary, combining ILS and MSMD one is able to tackle efficiently and reliably the problem of understanding the ligand migration process inside a protein, which is intimately linked to the its biological function.

Acknowledgments

Computer power was provided by the Centro de computacion de alto rendimiento (C.E.C.A.R.) at the FCEN-UBA and by the cluster MCG PME No 2006-01581 at the Universidad Nacional de Cordoba. F.F. and L.B. are fellowship from the Spanish MEC and the CONICET, respectively.

References

1. Ghosh, A. The Smallest Biomolecules: Diatomics and Their Interactions with Heme Proteins; The Netherlands: Elsevier, 2008.
2. Vinogradov, S. N.; Moens, L. J Biol Chem 2008, 283, 8773.
3. Wittenberg, J. B.; Wittenberg, B. A. J Exp Biol 2003, 206 (Part 12), 2011.
4. Scott, E. E.; Gibson, Q. H.; Olson, J. S. J Biol Chem 2001, 276, 5177.
5. Frauenfelder, H.; McMahon, B. H.; Austin, R. H.; Chu, K.; Groves, J. T. Proc Natl Acad Sci USA 2001, 98, 2370.
6. Megson, I. L.; Miller, M. R. Handb Exp Pharmacol 2009, 191, 247–276.
7. Boon, E. M.; Marletta, M. A. Curr Opin Chem Biol 2005, 9, 441.
8. Perutz, M. F.; Paoli, M.; Lesk, A. M. Chem Biol 1999, 6, R291.
9. Ibrahim, M.; Kuchinskas, M.; Youn, H.; Kerby, R. L.; Roberts, G. P.; Poulos, T. L.; Spiro, T. G. J Inorg Biochem 2007, 101, 1776.
10. Marti, M. A.; Gonzalez Lebrero, M. C.; Roitberg, A. E.; Estrin, D. A. J Am Chem Soc 2008, 130, 1611.
11. Andersen, J. F.; Ding, X. D.; Balfour, C.; Shokhireva, T. K.; Champagne, D. E.; Walker, F. A.; Montfort, W. R. Biochemistry 2000, 39, 10118.
12. Kondrashov, D. A.; Roberts, S. A.; Weichsel, A.; Montfort, W. R. Biochemistry 2004, 43, 13637.
13. Menyhárd, D. K.; Keserü, G. M. FEBS Lett 2005, 579, 5392.
14. Gilles-Gonzalez, M. A.; Gonzalez, G. J Inorg Biochem 2005, 99, 1.
15. Wittenberg, J. B.; Bolognesi, M.; Wittenberg, B. A.; Guertin, M. J Biol Chem 2002, 277, 871.
16. Nardini, M.; Pesce, A.; Milani, M.; Bolognesi, M. Gene 2007, 398, 2.
17. Pathania, R.; Navani, N. K.; Rajamohan, G.; Dikshit, K. L. J Biol Chem 2002, 277, 15293.
18. Bidon-Chanal, A.; Marti, M. A.; Crespo, A.; Milani, M.; Orozco, M.; Bolognesi, M.; Luque, F. J.; Estrin, D. A. Proteins 2006, 64, 457.
19. Boechi, L.; Marti, M. A.; Milani, M.; Bolognesi, M.; Luque, F. J.; Estrin, D. A. Proteins 2008, 73, 372.
20. Boechi, L.; Manez, P. A.; Luque, F. J.; Marti, M. A.; Estrin, D. A. Proteins 2010, 78, 962.
21. Nadra, A. D.; Martí, M. A.; Pesce, A.; Bolognesi, M.; Estrin, D. A. Proteins: Struct Funct Bioinformatics 2007, 71, 695.
22. Brunori, M.; Vallone, B. Cell Mol Life Sci 2007, 64, 1259.
23. Lama, A.; Pawaria, S.; Bidon-Chanal, A.; Anand, A.; Gelpi, J. L.; Arya, S.; Marti, M.; Estrin, D. A.; Luque, F. J.; Dikshit, K. L. J Biol Chem 2009, 284, 14457.
24. Bidon-Chanal, A.; Marti, M. A.; Estrin, D. A.; Luque, F. J. J Am Chem Soc 2007, 129, 6782.
25. Laverman, L. E.; Ford, P. C. J Am Chem Soc 2001, 123, 11614.
26. Milani, M.; Pesce, A.; Nardini, M.; Ouellet, H.; Ouellet, Y.; Dewilde, S.; Bocedi, A.; Ascenzi, P.; Guertin, M.; Moens, L.; Friedman, J. M.; Wittenberg, J. B.; Bolognesi, M. J Inorg Biochem 2005, 99, 97.
27. Marti, M. A.; Crespo, A.; Capece, L.; Boechi, L.; Bikiel, D. E.; Scherlis, D. A.; Estrin, D. A. J Inorg Biochem 2006, 100, 761.
28. Marti, M. A.; Estrin, D. A.; Roitberg, A. E. J Phys Chem B 2009, 113, 2135.
29. Swails, J. M.; Meng, Y.; Walker, F. A.; Marti, M. A.; Estrin, D. A.; Roitberg, A. E. J Phys Chem B 2009, 113, 1192.
30. Pesce, A.; Milani, M.; Nardini, M.; Bolognesi, M. In Methods in Enzymology, The Netherlands: Elsevier; 2008, pp. 303–315.
31. De Sanctis, D.; Dewilde, S.; Pesce, A.; Moens, L.; Ascenzi, P.; Hankeln, T.; Burmester, T.; Bolognesi, M. Biochem Biophys Res Commun 2004, 316, 1217.
32. Milani, M.; Pesce, A.; Ouellet, Y.; Dewilde, S.; Friedman, J.; Ascenzi, P.; Guertin, M.; Bolognesi, M. J Biol Chem 2004, 279, 21520.
33. Simmerling, C.; Strockbine, B.; Roitberg, A. E. J Am Chem Soc 2002, 124, 11258.
34. Hassan, S. A.; Gracia, L.; Vasudevan, G.; Steinbach, P. J. Methods Mol Biol 2005, 305, 451.
35. Domene, C.; Doyle, D. A.; Venien-Bryan, C. Biophys J 2005, 89, L01.
36. Friesner, R. A.; Guallar, V. Annu Rev Phys Chem 2005, 56, 389.
37. Bossa, C.; Anselmi, M.; Roccatano, D.; Amadei, A.; Vallone, B.; Brunori, M.; Di Nola, A. Biophys J 2004, 86, 3855.
38. Ruscio, J. Z.; Kumar, D.; Shukla, M.; Prisant, M. G.; Murali, T. M.; Onufriev, A. V. Proc Natl Acad Sci USA 2008, 105, 9204.
39. Nutt, D. R.; Meuwly, M. Proc Natl Acad Sci USA 2004, 101, 5998.
40. Lutz, S.; Nienhaus, K.; Nienhaus, G. U.; Meuwly, M. J Phys Chem B 2009, 113, 15334.
41. Nishihara, Y.; Hayashi, S.; Kato, S. Chem Phys Lett 2008, 464, 220.
42. Arroyo-Mañez, P.; Bikiel, D. E.; Boechi, L.; Capece, L.; Di Lella, S.; Estrin, D. A.; Martí, M. A.; Moreno, D. M.; Nadra, A. D.; Petruk, A. A. Biochim Biophys Acta 2010.
43. Kalko, S. G.; Gelpi, J. L.; Fita, I.; Orozco, M. J Am Chem Soc 2001, 123, 9665.

44. Guallar, V.; Lu, C.; Borrelli, K.; Egawa, T.; Yeh, S. R. J Biol Chem 2009, 284, 3106.
45. Carrillo, O.; Orozco, M. Proteins: Struct Funct Genet 2008, 70, 892.
46. Baron, R.; Riley, C.; Chenprakhon, P.; Thotsaporn, K.; Winter, R. T.; Alfieri, A.; Forneris, F.; van Berkel, W. J. H.; Chaiyen, P.; Fraaije, M. W.; Mattevi, A.; McCammon, J. A. Proc Natl Acad Sci 2009, 106, 10603.
47. Orlowski, S.; Nowak, W. Biosystems 2008, 94, 263.
48. Cohen, J.; Olsen, K. W.; Schulten, K. Methods Enzymol 2008, 437, 439.
49. Golden, S. D.; Olsen, K. W. Methods Enzymol 2008, 437, 417.
50. Jarzynski, C. Phys Rev Lett 1997, 78, 2690.
51. Xiong, H.; Crespo, A.; Marti, M.; Estrin, D.; Roitberg, A. E. Theor Chem Acc 2006, 116, 338.
52. Crespo, A.; Marti, M. A.; Estrin, D. A.; Roitberg, A. E. J Am Chem Soc 2005, 127, 6940.
53. Amara, P.; Andreoletti, P.; Jouve, H. M.; Field1, M. J. Protein Sci 2001, 10, 1927.
54. Gervasio, F. L.; Laio, A.; Parrinello, M. J Am Chem Soc 2004, 127, 2600.
55. Bocahut, A.; Bernad, S.; Sebban, P.; Sacquin-Mora, S. J Phys Chem B 2009, 113, 16257.
56. Ouellet, H.; Milani, M.; LaBarre, M.; Bolognesi, M.; Couture, M.; Guertin, M. Biochemistry 2007, 46, 11440.
57. Jarzynski, C. Phys Rev E 1997, 56, 5018.
58. Hummer, G.; Szabo, A. PNAS 2001, 98, 3858.
59. Mills, M.; Andricioael, I. J Chem Phys 2008, 129, 114101.
60. Hornak, V.; Abel, R.; Okur, A.; Strockbine, B.; Roitberg, A.; Simmerling, C. Proteins: Struct Funct Genet 2006, 65, 712.
61. Pearlman, D. A.; Case, D. A.; Caldwell, J. W.; Ross, W. S.; Cheatham Iii, T. E.; DeBolt, S.; Ferguson, D.; Seibel, G.; Kollman, P. Comput Phys Commun 1995, 91, 1.
62. Milani, M.; Pesce, A.; Ouellet, Y.; Ascenzi, P.; Guertin, M.; Bolognesi, M. EMBO J 2001, 20, 3902.
63. Ouellet, H.; Ouellet, Y.; Richard, C.; Labarre, M.; Wittenberg, B.; Wittenberg, J.; Guertin, M. Proc Natl Acad Sci USA 2002, 99, 5902.
64. Dantsker, D.; Samuni, U.; Ouellet, Y.; Wittenberg, B. A.; Wittenberg, J. B.; Milani, M.; Bolognesi, M.; Guertin, M.; Friedman, J. M. J Biol Chem 2004, 279, 0021.
65. Maes, E. M.; Roberts, S. A.; Weichsel, A.; Montfort, W. R. Biochemistry 2005, 44, 12690.
66. Burendahl, S.; Danciulescu, C.; Nilsson, L. Proteins: Struct Funct Bioinformatics 2009, 77, 842.